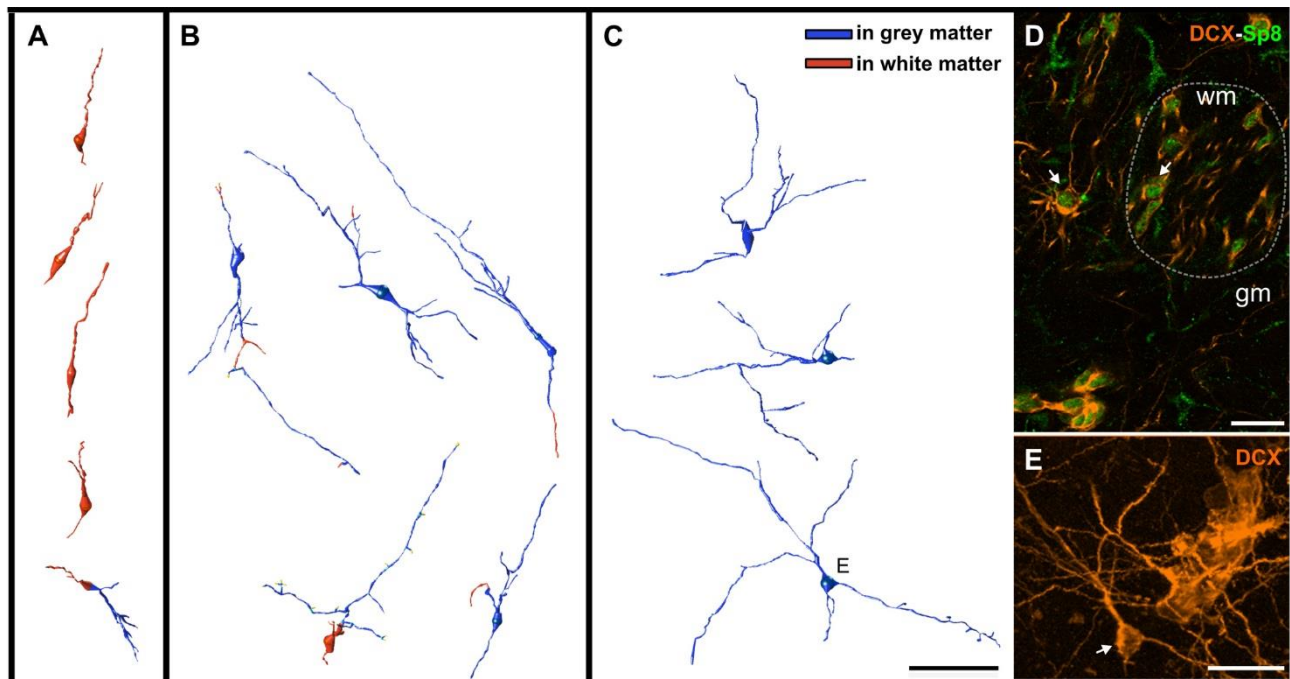
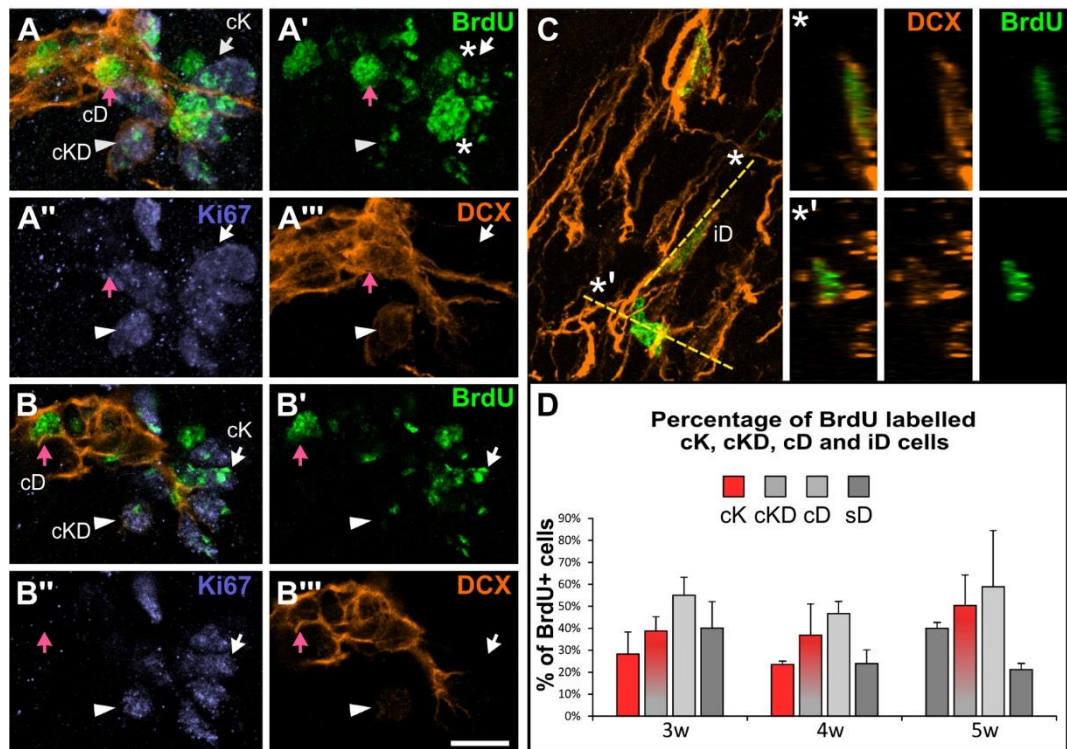


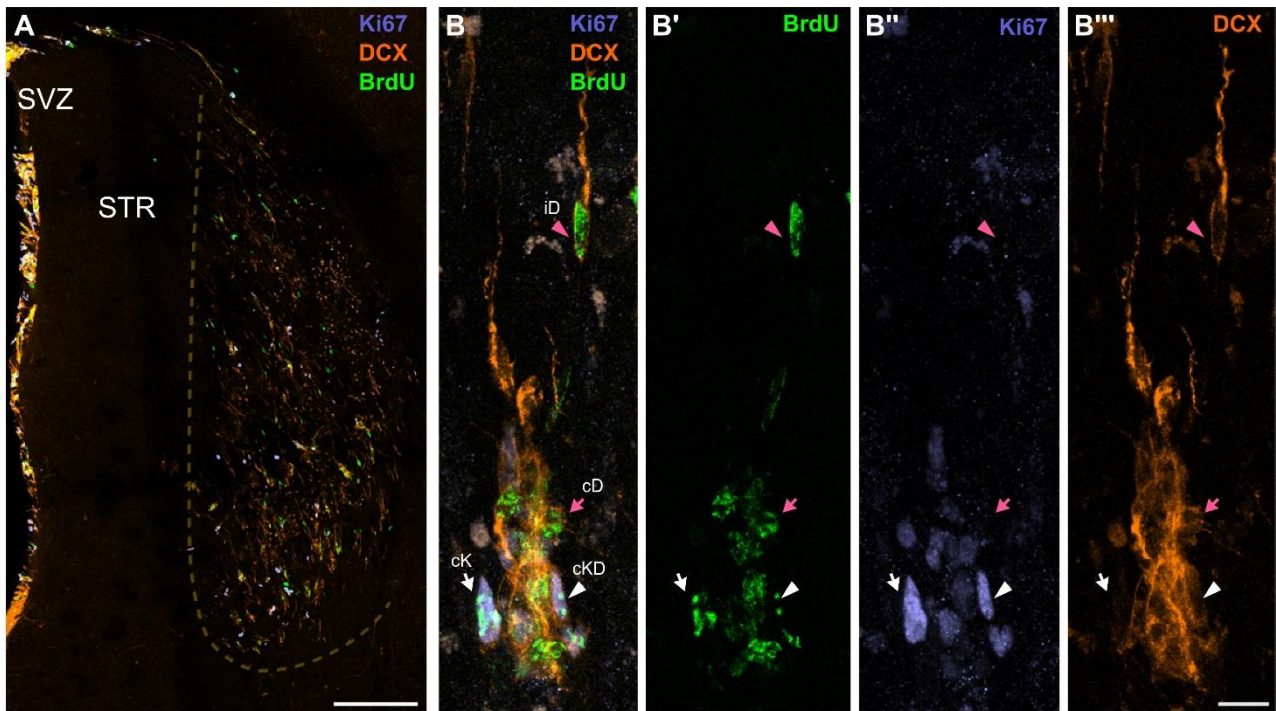
Supplementary Figures



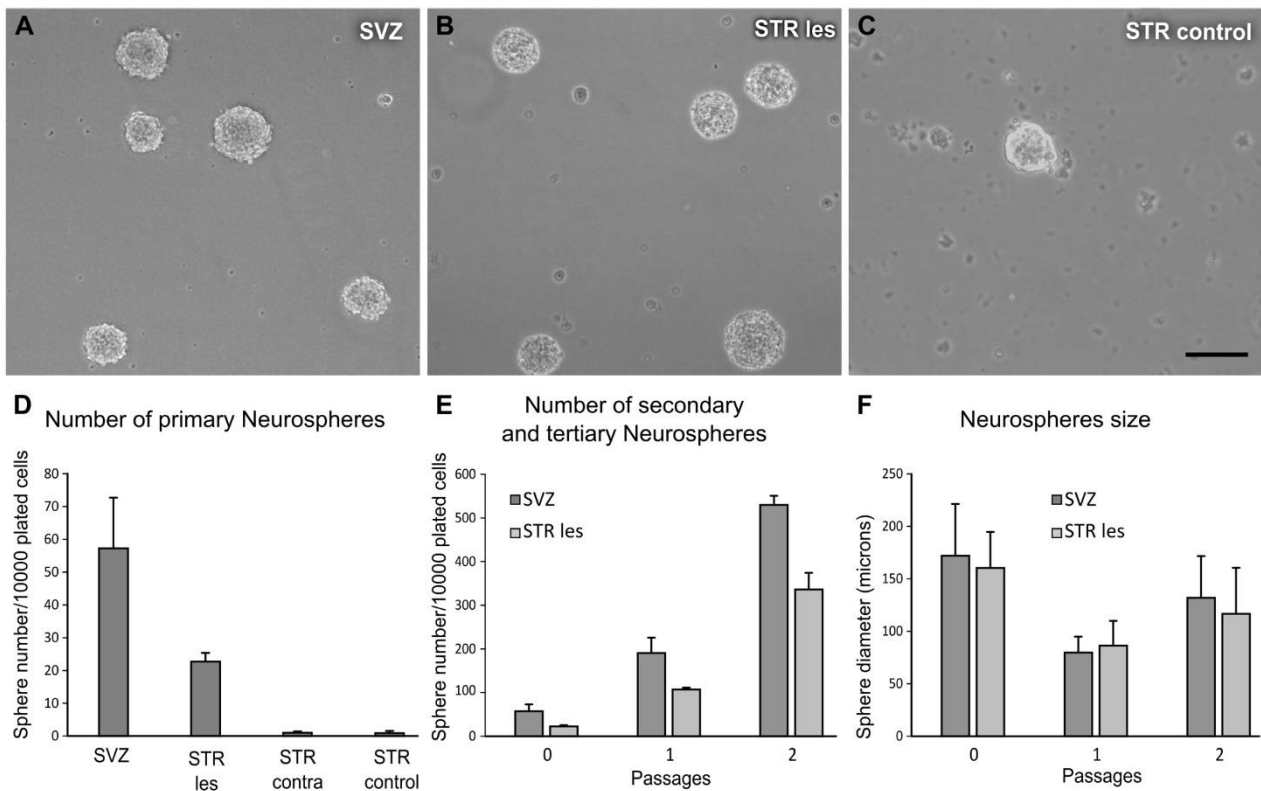
Supplementary Fig.1) Phenotypic analysis of DCX^+ cells in the 5w.p.l striatum. **a-c)** Threedimensional reconstructions of DCX^+ neuroblasts. According with their complexity and with the presence of processes in the grey (blue) and white (red) matter we divided these cells in three categories. **a)** Cells with short unbranched processes: most such cells were associated with the white matter and showed the characteristic bipolar morphology of migrating neuroblasts. **b)** Cells with long and branched processes running in both white and grey matter. **c)** Cells with long and branched processes running exclusively in the grey matter. It is to note that although most cells associated mainly with the white matter were bipolar, some showed a more elaborated morphology. However, these few cells were surrounded by a high density of cells and processes that hampered the complete reconstruction of their morphology. **d)** Single confocal slice showing the expression of SP8 (green) in DCX^+ cells (orange). Note that this transcription factors is expressed in both cD (arrowhead) and iD (arrows) cells in both grey and white matter (dotted line). **e)** Z projection of part of the stack containing one of the reconstructed cells (arrow) shown in **d**. Scale Bars: 40 μ m in **a-c**, 20 μ m in **d,e**.



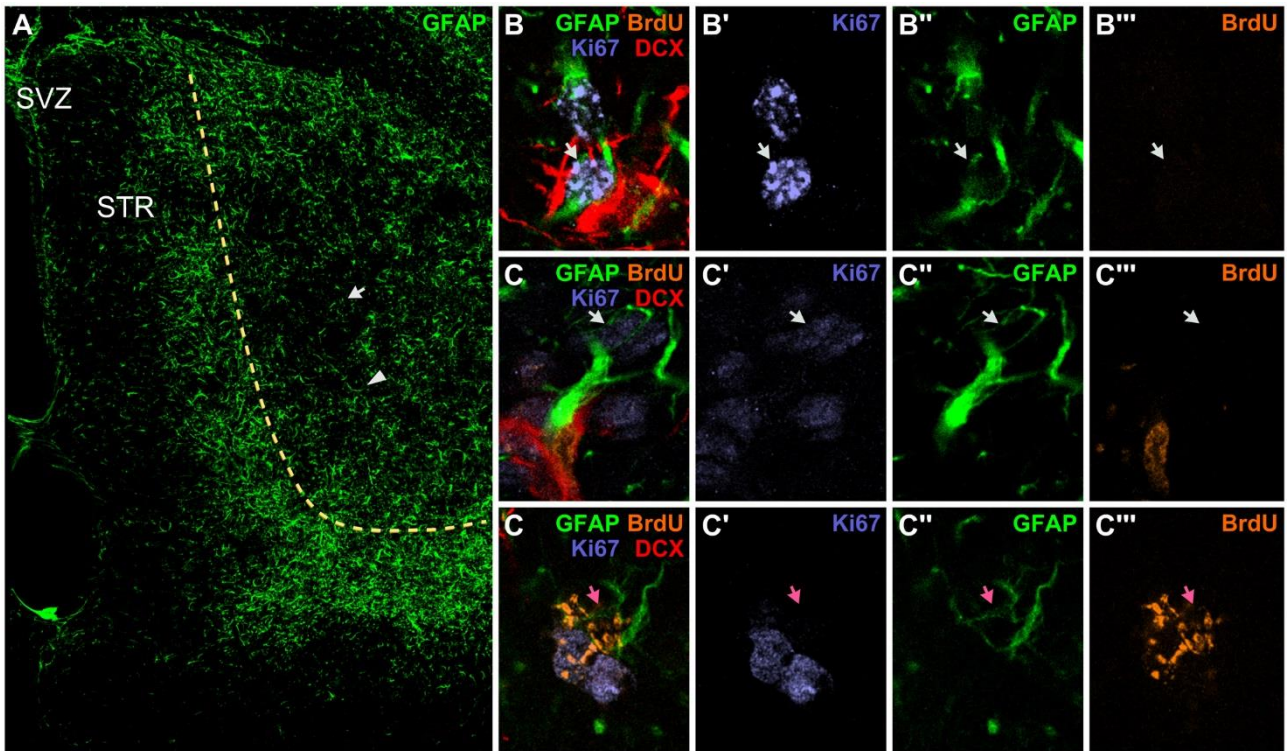
Supplementary Fig.2) BrdU labelling among induced striatal $Ki67^+$ clusters and DCX^+ neuroblasts. **a-b)** Zprojection (**b-b'''**) and single confocal plane (**c-c'''**) of a $Ki67^+$ (violet) cluster partially overlapped with a DCX^+ (orange) cluster showing examples of cK (white arrow), cKD (white arrowhead) and cD (pink arrow) cells labelled by BrdU, four days after administration (green). The fragmented BrdU staining in the $Ki67^+$ cells suggests that these cells are actively dividing. **c)** Some individual DCX^+ cells (iD) are also labelled for BrdU (pink arrowhead). For two such cells a reslice along the plane indicated by a dotted line is indicated (*, *'). **d)** Percentages \pm S.D. of BrdU+ cells among cK, cKD, cD and iD cells cells at 3, 4, 5w.p.i., n=4. Error bars indicate standard deviation. Scale bars: 10 μ m.



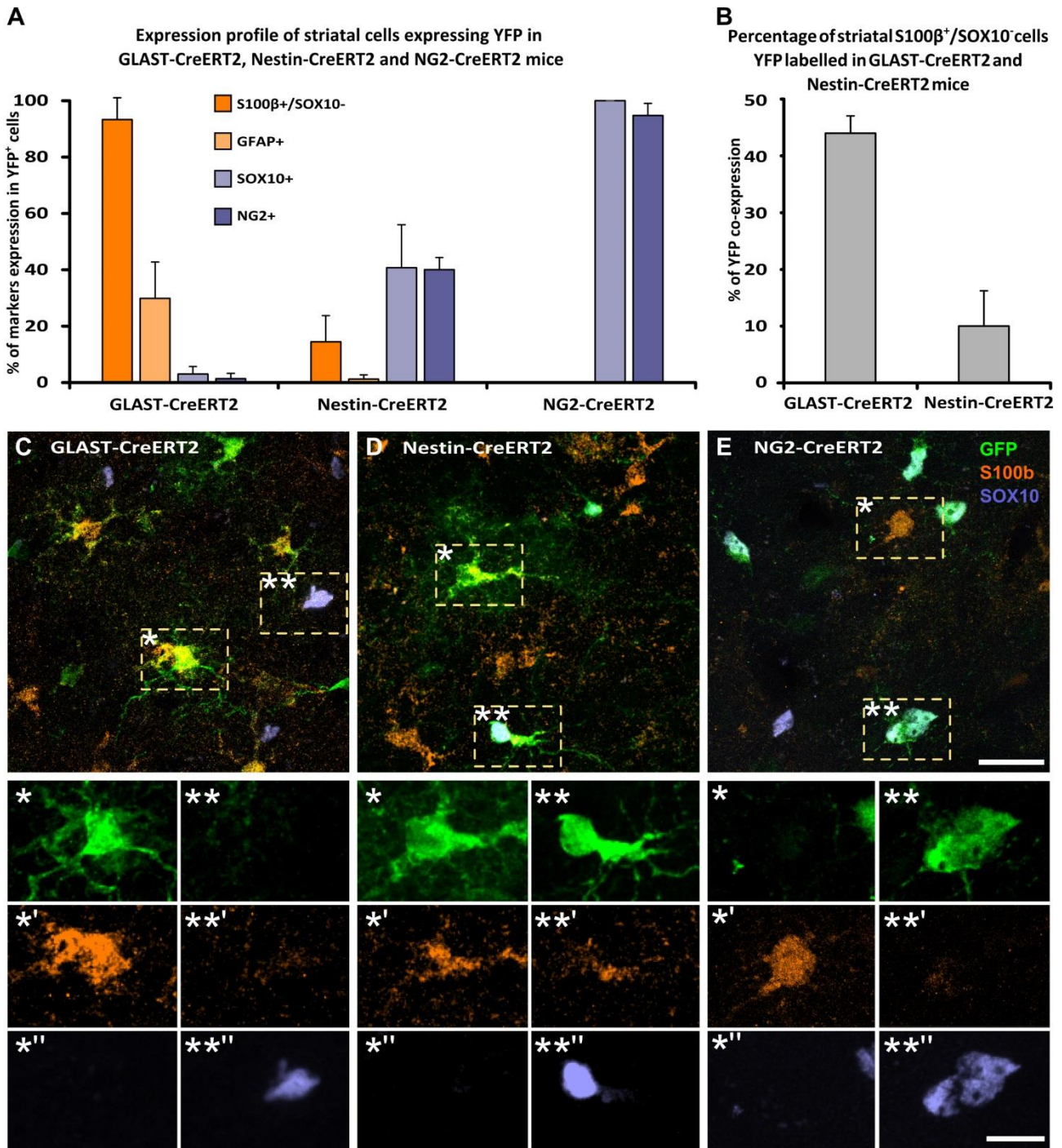
Supplementary Fig.3) The QA lesion induces a long lasting neurogenic response. **a**) Coronal section of an animal sacrificed 6 month after QA lesion showing striatal Ki67⁺ (violet) and DCX⁺ (orange) cells in the striatum, mostly located within the lesioned area (yellow dotted line). Several Ki67⁺ and DCX⁺ cells incorporated the BrdU (green) injected four days before the sacrifice. **b-b''**) Confocal stack showing an higher magnification of Ki67 and DCX⁺ cells in the lesioned striatum. These cells include a cluster of cK (white arrow), cKD (white arrowhead) and cD (pink arrow) cells as well as iD (pink arrowhead) cells. Note that all cell types are partly labelled for BrdU. Scale bars: 200µm in **a**; 10µm in **b-b'**.



Supplementary Fig.4) Neurosphere assay. **a-c)** Representative images of primary neurospheres isolated from intact SVZ (**a**), lesioned striatum (STR les; **b**), and intact striatum (STR control; **c**). **d)** Number of primary neurospheres isolated from SVZ, lesioned striatum, striatum contralateral to the QA injection (STR contra) and intact striatum from non lesioned animals of a representative experiment. Bars indicate the mean values \pm S.E.M. of the number of neurospheres for 10000 plated cells; n=4 dishes for each case). **e)** The number of SVZ and STR les derived neurospheres steeply increase during the first two *in vitro* passages while the neurospheres diameter remain constant (**f**). Scale bar: 150 μ m.

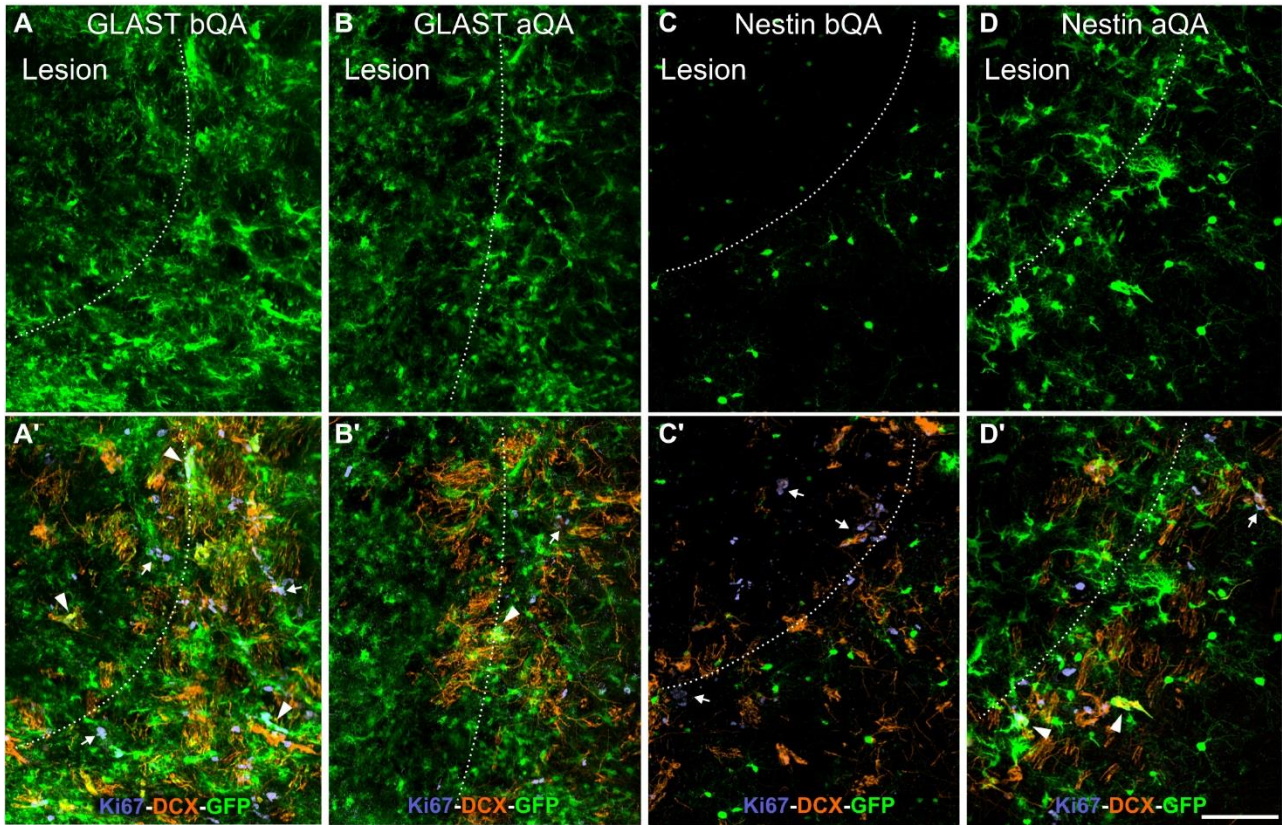


Supplementary Fig.5) Proliferation of striatal GFAP⁺ astrocytes. a) Coronal section of a 5w.p.l. striatum showing the staining of GFAP (green). In contrast to control animals, GFAP is strongly expressed by striatal astrocytes after lesion, particularly at the lesion border (dotted line). b) Single confocal plane showing a GFAP⁺ (green) cell labelled by Ki67⁺ (violet) but not DCX (red) nor BrdU (orange; white arrow). Note that this cell is close to a second Ki67⁺ cells in which the positivity for GFAP cannot be clearly established. c) Single confocal plane showing a GFAP⁺ cell labelled by Ki67⁺ in a cluster comprising cK (white arrow), cKD and cD cells. d) Single confocal plane showing a GFAP⁺ cell labelled by BrdU (pink arrow). This cell was closely associated to a cluster of cK cells (two of which are visible in this focal plane) that were also mostly labelled for BrdU. Scale Bars: 200 μ m in a, 10 μ m in b-d.

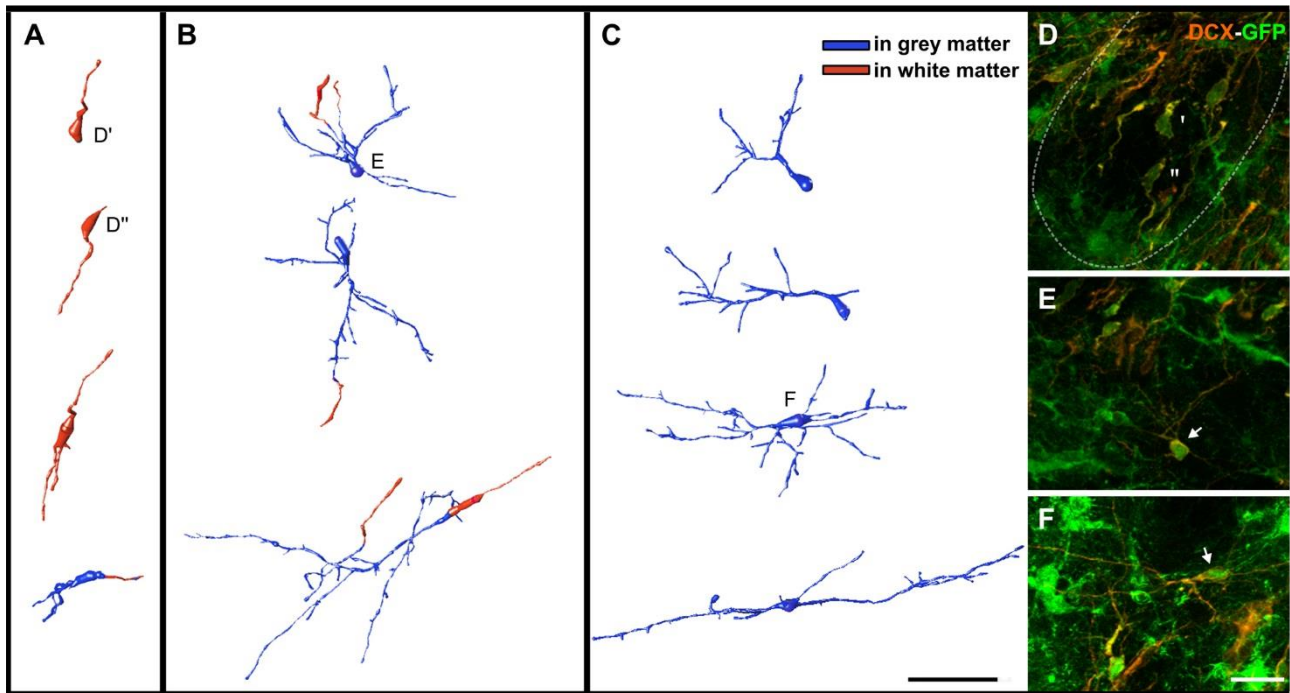


Supplementary Figure 6) Phenotypic analysis of recombined cells in the intact striatum of GLAST, Nestin and NG2-CreER^{T2} animals. **a**) Percentage of YFP⁺ cells expressing markers of the astroglial (S100β, GFAP) or oligodendroglial (NG2, SOX10) lineages in the intact striatum of GLAST, Nestin and NG2-CreER^{T2} animals either one week (for GLAST-CreER^{T2} and Nestin-CreER^{T2}) or two weeks (for NG2) after tamoxifen administration. Since part of the S100β cells co-expressed SOX10, only the S100β⁺/SOX10⁻ cells were considered as astroglia. As expected, YFP⁺ cells were almost exclusively represented by astrocytes in GLASTCreER^{T2} animals, by a mixture of astroglial and oligodendroglial cells in Nestin-CreER^{T2} animals and exclusively by oligodendroglial cells in NG2-CreER^{T2} animals. It is to note that only a small percentage of YFP⁺ cells co-express GFAP, and this is consistent with the low expression of this protein in the intact parenchyma. **b**) Fraction of recombined S100β⁺/SOX10⁻ astrocytes in GLAST-CreER^{T2} and Nestin-CreER^{T2} animals. **c-d**)

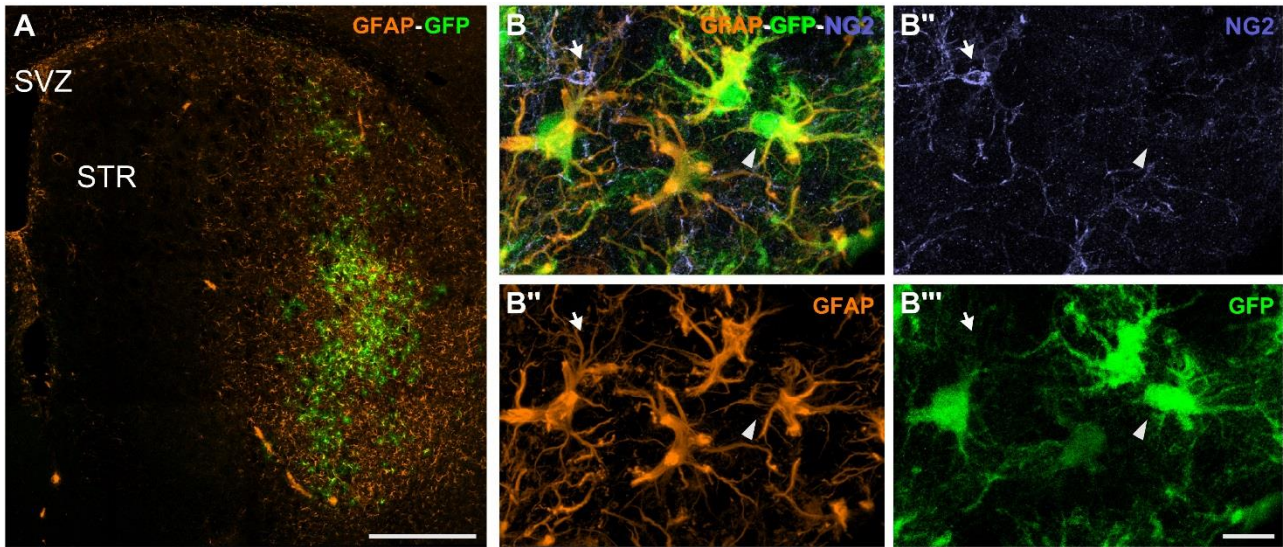
Confocal stacks of the intact striatum of GLAST-CreER^{T2} (c), NestinCreER^{T2} (d) and NG2-CreER^{T2} mice (e) showing the expression YFP (green) in S100 β ⁺ (orange, *) or SOX10⁺ (violet, **) cells. Note that the expression of SOX10 or S100 β in YFP⁺ cells closely correlate with the occurrence of morphological features characteristic of the oligodendroglial or astroglial lineages, respectively. Error bars indicate standard deviation. Scale bars: 20 μ m in **b**, **c**, **d**; 10 μ m in higher magnifications



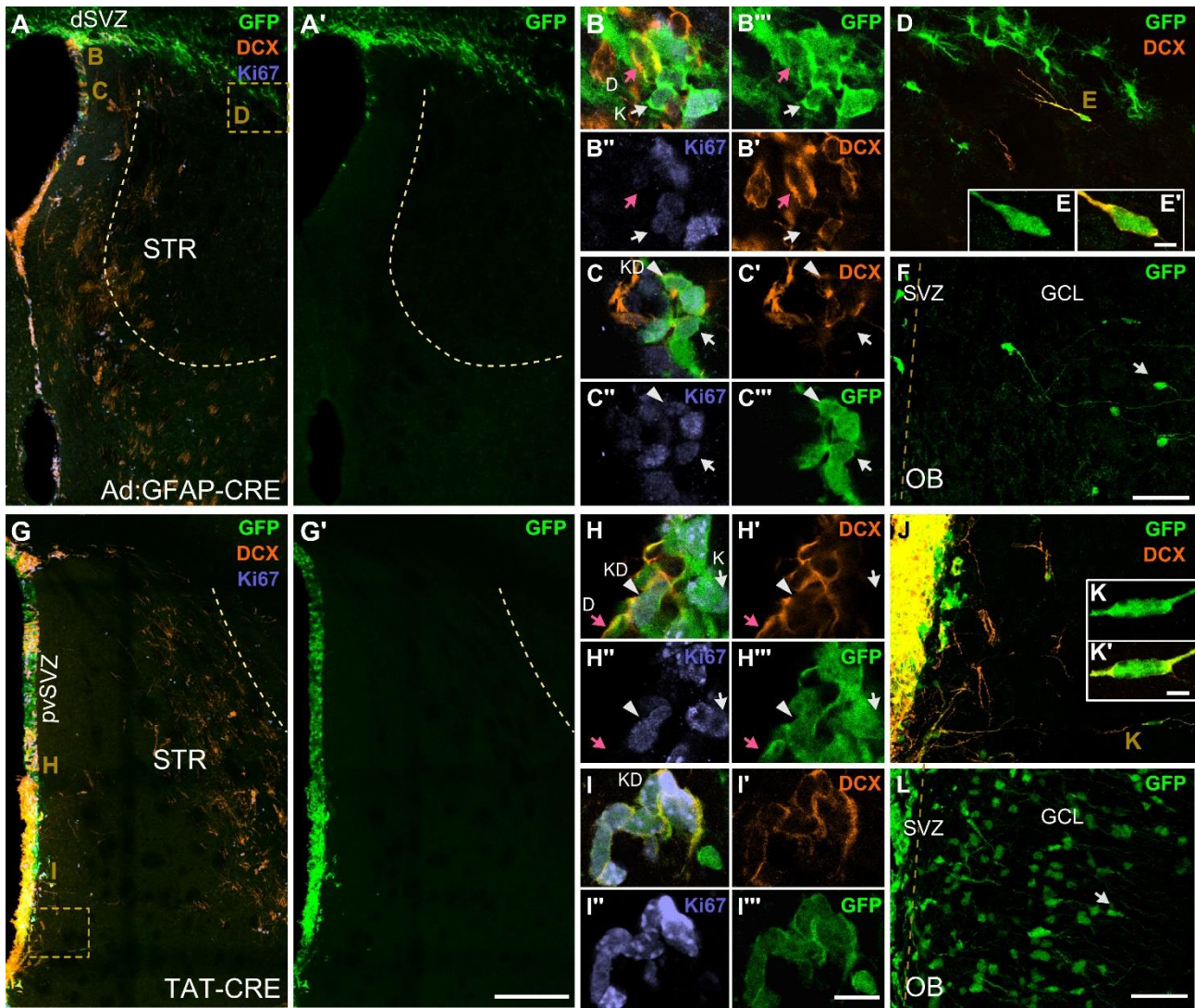
Supplementary Fig.7) *Distribution of YFP⁺ cells in the striatum of fate mapped animals. ad*) YFP (green) Ki67 (violet) and DCX (orange) staining in representative 50 μ m coronal sections of 5w.p.l. striatum at the level of the lesion border (dotted line) of GLAST-CreER^{T2} bQA (**a,a'**), GLAST-CreER^{T2} aQA (**b,b'**), Nestin-CreER^{T2} bQA (**c,c'**) and Nestin-CreER^{T2} aQA animals. Note that numerous GFP⁺ cells can be observed at the lesion border of both GLAST-CreER^{T2} bQA and aQA animals. By contrast, in Nestin-CreER^{T2} bQA animals only few YFP⁺ cells can be observed, and according to their characteristic morphology these elements represent mostly oligodendrocytes and to a lesser extent neurons. Similar cells can be observed also in Nestin-CreER^{T2} aQA animals together with numerous cells with astrocytic morphology mostly distributed at the lesion border, where most Ki67⁺ and DCX⁺ clusters were located. In **a'-d'** also note that only a fraction of Ki67⁺ clusters contains GFP⁺ cells (arrowhead and arrow indicate respectively recombined and non recombined Ki67⁺ clusters). Scale bar: 100 μ m.



Supplementary Figure 8) Three dimensional reconstruction of DCX^+/YFP^+ cells in the 5w.p.l striatum of $GLAST-CreER^{T2}$ bQA animals **a-c)** Three-dimensional reconstructions of DCX^+ neuroblasts that expressed YFP in the 5w.p.l striatum of $GLAST-CreER^{T2}$ animals treated with tamoxifen one week before QA lesion. The morphology of these cells were consistent with the categories of DCX^+ neuroblasts previously described in supplementary Fig.1 **d-f)** Z projection of part of the stack containing some of the reconstructed cells shown in **a-c)**. Scale Bars: 40 μ m in **a-c)**, 20 μ m in **d, e)**.



Supplementary Fig.9) Phenotypic analysis of recombined cells in the intact striatum of R26R animals receiving Ad:GFAP-Cre injections. a) Coronal section at the level of the striatum labelled for GFAP (orange) and GFP (green). Note that the GFP⁺ cells are restricted to the ventro-lateral striatum and that the injection of the viral vector consistently induced the expression of GFAP at the level of the injection site and surrounding area of the striatum. The reactivity of astrocytes is consistent with previous work showing that intracerebral injections of adenoviral vectors induce an inflammatory response (Lowenstein and Castro, 2003). *b)* Z-Projection of a confocal stack at the level of the injection site showing that recombined cells expressing YFP (green) co-express GFAP (orange, arrowhead) but not NG2 (violet, arrow). Quantitative analyses indicated that no YFP⁺ cells in the striatum of these animals expressed NG2 and the 93±5% (n=3) expressed GFAP. Scale Bars: 200 µm in **a**, 20 µm in **b**.



Supplementary Fig.10) SVZ contribution to QA lesion induced neurogenesis. a-f) Coronal sections at the level of the central striatum (a, and higher magnifications in b-d) and olfactory bulb (f) of a 5w.p.l R26R reporter mice injected with Ad:GFAP-Cre one week before QA. **g-l)** coronal sections at the level of the anterior striatum (g, and higher magnifications in h-j) and olfactory bulb (l) of a 5w.p.l R26R reporter mice injected with TAT-Cre one week before QA. The injection of the Ad:GFAP-Cre and TAT-Cre induced widespread expression of YFP (green) respectively in in the dorso-lateral parts of the SVZ (dSVZ, a) and its peri-ventricular regions (pvSVZ, g). As shown by higher magnification of single confocal planes, YFP⁺ cells in both the dSVZ (b) and pvSVZ (c,h) include putative TAPs expressing Ki67 (violet) but not DCX (orange, white arrow), as well as proliferating (white arrowhead) and post-mitotic (pink arrow) DCX⁺ neuroblasts. In addition for both injection protocols many YFP⁺ cells could be observed in the OB (white arrows) f,l). Collectively these observations indicate that our approach consistently labelled longlasting primary neuronal progenitors of all SVZ sub-regions. Nonetheless in the striatum of these animals we could identify only few YFP⁺ iD cells (d, e and j, k) and these cells were generally located within 200µm from the SVZ. It is to note that a few clusters of Ki67⁺ and YFP⁺ cells were occasionally observed in TAT-Cre injected animals (i), particularly at anterior levels of the striatum. However these clusters were mostly made by cKD cells and were always located at less than 50µm from the SVZ. Scale Bars 200µm in a-g, 50 µm in d, f, j, l, 10 µm in b, c, ,h, l, 5 µm in e-k.

Supplementary Table 1) Analysis of *YFP* expression in *Ki67⁺* and *DCX⁺* cells in the SVZ and striatum of *GLAST* and *Nestin-CreER^{T2}* animals, in *bQA* and *aQA* condition.

In the table are reported the values of statistical tests performed on the percentage of *YFP⁺* cells among different striatal (STR) and SVZ cell types shown in Fig.2a. For ANOVA analyses that returned statistically significant values, tukey post-hoc tests are also shown. **a) Within region comparisons.** Percentage of *YFP⁺* cells among distinct cell types is compared within the SVZ and STR. Note that in both *GLAST-CreER^{T2}* *bQA* and *Nestin-CreER^{T2}* *bQA* animals the fraction of *YFP⁺* elements among the considered cell types in each region is not statistically different. By contrast, in *GLAST-CreER^{T2}* *aQA* animals, in both SVZ and STR, the proliferating cells (SVZ: *Ksvz*, *KDsvz*; STR: *cK*, *cKD*) show a higher value of *YFP* coexpression in respect to postmitotic elements (SVZ: *Dsvz*; STR: *cD*, *iD*; see Fig.2A). *Nestin-CreER^{T2}* *aQA* animals show a similar trend, although in both SVZ and STR only the *Ki67⁺/DCX* cells (SVZ: *Ksvz*; STR: *cK*) contain a significantly higher fraction of *YFP⁺* cells. **b) Between regions comparisons.** The different cell types are compared between SVZ and STR. Note that in *GLAST-CreER^{T2}* *bQA* animals *cK*, *cKD* and *cD* cells show lower percentage of recombination in respect to the corresponding cell types in the SVZ (*Ksvz*, *KDsvz* and *Dsvz*). possibly due to different efficiency of *GLAST*-driven recombination among SVZ and striatal astrocytes. **c) Between groups comparisons.** The fraction of *YFP⁺* cells for all considered cell types is compared before and after tamoxifen among different strains (*GLAST-CreER^{T2}* *bQA* vs *Nestin-CreER^{T2}* *bQA*; *GLAST-CreER^{T2}* *aQA* vs *Nestin-CreER^{T2}* *aQA*), or in the same strain (*Nestin-CreER^{T2}* *bQA* vs *Nestin-CreER^{T2}* *aQA*; *GLAST-CreER^{T2}* *bQA* vs *GLAST-CreER^{T2}* *aQA*). Note that in the SVZ the percentage of *YFP⁺* cells does not differ between strains, indicating similar efficiency of *Nestin*- or *GLAST*-driven recombination in primary progenitors. By contrast, in the striatum all cell types show higher level of recombination in *GLAST-CreER^{T2}* *bQA* than in *Nestin-CreER^{T2}* *bQA* animals. This difference is lost in the *aQA* condition, accordingly to the significant increase of *cK* and *cKD* cells in *Nestin-CreER^{T2}* *aQA*, in respect to *Nestin-CreER^{T2}* *bQA* animals.

a) Within Regions Comparisons

| | Compared Cell types | STATISTICAL TEST | GLAST-bQA | Nestin-bQA | GLAST-aQA | Nestin-aQA |
|-----|---|------------------|--------------------------------------|---------------------------------------|---------------------------------------|---------------------------------------|
| SVZ | K_{SVZ} vs KD_{SVZ} vs D_{SVZ} | One way ANOVA | F _(2,6) =0,342 p=0,723 | F _(2,9) =1,432 p=0,288 | F _(2,6) =21,734 p=0,002 | F _(3,12) =5,597 p=0,012 |
| | <i>K_{SVZ} vs KD_{SVZ}</i> | Tukey post hoc | | | p=0,051 | p=0,024 |
| | <i>K_{SVZ} vs D_{SVZ}</i> | Tukey post hoc | - | - | p=0,001 | p=0,026 |
| | <i>KD_{SVZ} vs D_{SVZ}</i> | Tukey post hoc | | | p=0,028 | p=0,998 |
| STR | cK vs cKD vs cD vs iD | One way ANOVA | F _(3,8) =2,032 p=0,188 | F _(3,12) =2,713 p=0,092 | F _(3,8) =9,802 p=0,005 | F _(3,12) =5,597 p=0,012 |
| | <i>cK vs cKD</i> | Tukey post hoc | | | p=1,000 | p=0,076 |
| | <i>cK vs cD</i> | Tukey post hoc | | | p=0,027 | p=0,020 |
| | <i>cK vs iD</i> | Tukey post hoc | - | - | p=0,016 | p=0,036 |
| | <i>cKD vs cD</i> | Tukey post hoc | | | p=0,027 | p=0,670 |
| | <i>cKD vs iD</i> | Tukey post hoc | | | p=0,016 | p=0,849 |
| | <i>cD vs iD</i> | Tukey post hoc | | | p=0,979 | p=0,990 |

b) Between Regions Comparisons

| | Compared Cell types | STATISTICAL TEST | GLAST-bQA | Nestin-bQA | GLAST-aQA | Nestin-aQA |
|------------|--|------------------|---------------------------------------|---------------------------------------|--------------------------------------|--------------------------------------|
| STR vs SVZ | K_{SVZ} vs cK_{SVZ} | T-Test | p=0,038 | p<0,001 | p=0,020 | p=0,372 |
| | KD_{SVZ} vs cKD | T-Test | p=0,016 | p=0,001 | p=0,380 | p=1,000 |
| | D_{SVZ} vs cD vs iD | One way ANOVA | F _(2,6) =10,599 p=0,011 | F _(2,9) =35,737 p<0,001 | F _(2,6) =3,198 p=0,113 | F _(2,6) =1,960 p=0,221 |
| | <i>D_{SVZ} vs cD</i> | Tukey post hoc | p=0,009 | p<0,001 | | |
| | <i>D_{SVZ} vs iD</i> | Tukey post hoc | p=0,189 | p<0,001 | - | - |
| | <i>cD vs iD</i> | Tukey post hoc | p=0,092 | p=0,409 | | |

c) Between Groups Comparisons

| | Compared Cell types | STATISTICAL TEST | GLAST-bQA vs Nestin-bQA | GLAST-aQA vs Nestin-aQA | GLAST-bQA vs GLAST-aQA | Nestin-bQA vs Nestin-aQA |
|-----|-------------------------|------------------|-------------------------|-------------------------|------------------------|--------------------------|
| SVZ | K_{SVZ} | T-Test | p=0,110 | p=0,142 | p=0,019 | p=0,030 |
| | KD_{SVZ} | T-Test | p=0,068 | p=0,049 | p=0,004 | p<0,001 |
| | D_{SVZ} | T-Test | p=0,899 | p=0,577 | p<0,001 | p<0,001 |
| STR | ck | T-Test | p=0,002 | p=0,477 | p=0,060 | p=0,015 |
| | cKD | T-Test | p=0,049 | p=0,153 | p=0,241 | p=0,030 |
| | cD | T-Test | p=0,010 | p=0,838 | p=0,017 | p=0,605 |
| | iD | T-Test | p=0,015 | p=0,069 | p=0,011 | p=0,298 |

Table S2. Antibodies

| ANTIGEN NAME | HOST | DILUTION | SOURCE | STOCK NUMBER |
|---------------------------|---------|----------|--------------------------|--------------|
| <i>Primary antisera</i> | | | | |
| ASCL-1 | Mouse | 1:500 | BD Pharmingen | 556604 |
| BrdU | Rat | 1:3000 | AbD Serotec | OBT0030CX |
| DCX | Goat | 1:1500 | Santa Cruz Biotechnology | Sc-8066 |
| GFAP | Rabbit | 1:2000 | Dako | Z 0334 |
| GFP | Chicken | 1:1000 | Aveslab | GFP-1020 |
| Ki67 | Rabbit | 1:1000 | Novocastra | NCL-Ki67p |
| Ki67 | Mouse | 1:500 | BD Pharmingen | 550609 |
| NeuN | Mouse | 1:1000 | Chemicon | MAB377 |
| NG2 | Rabbit | 1:500 | Chemicon | AB5320 |
| O4 | Mouse | 1:200 | Millipore | MAB345 |
| S100 β | Rabbit | 1:10000 | Swant | 37A |
| SOX-10 | Goat | 1:1000 | Santa Cruz Biotechnology | Sc-17342 |
| SOX-9 | Rabbit | 1:1000 | Millipore | AB5535 |
| Sp8 | Rabbit | 1:10000 | Millipore | AB15260 |
| Tuj1 | Mouse | 1:1500 | Sigma | T8660 |
| <i>Secondary antisera</i> | | | | |
| Cy3 Anti-Rb | Donkey | 1:800 | Jackson ImmunoResearch | 711-165-152 |
| Cy3 Anti-Ms | Donkey | 1:800 | Jackson ImmunoResearch | 715-165-151 |
| Cy3 Anti-Gt | Donkey | 1:800 | Jackson ImmunoResearch | 705-165-147 |
| Cy3 Anti-Rt | Donkey | 1:800 | Jackson ImmunoResearch | 712-165-153 |
| AlexaFluor488 Anti-Rb | Donkey | 1:400 | Jackson ImmunoResearch | 711-545-152 |
| AlexaFluor488 Anti-Ms | Donkey | 1:400 | Jackson ImmunoResearch | 715-545-151 |
| AlexaFluor488 Anti-Gt | Donkey | 1:400 | Jackson ImmunoResearch | 705-545-147 |
| AlexaFluor488 Anti-Rt | Donkey | 1:400 | Jackson ImmunoResearch | 712-545-153 |
| AlexaFluor488 Anti-Ck | Donkey | 1:400 | Jackson ImmunoResearch | 703-545-155 |
| AlexaFluor647 Anti-Rb | Donkey | 1:600 | Jackson ImmunoResearch | 711-605-152 |
| AlexaFluor647 Anti-Ms | Donkey | 1:600 | Jackson ImmunoResearch | 715-605-151 |
| AlexaFluor647 Anti-Gt | Donkey | 1:600 | Jackson ImmunoResearch | 705-605-147 |
| AlexaFluor647 Anti-Rt | Donkey | 1:600 | Jackson ImmunoResearch | 712-605-153 |
| Biotynilated Anti-Rat | Rabbit | 1:150 | Vector Laboratories | BA-4001 |
| AMCA-avidinD | | 1:100 | Vector Laboratories | A-2008 |

Supplementary materials and methods

Transgenic Mouse lines

Experiments were performed on 8-12 weeks animals of the following mouse lines: C57BL/6 mice (Harlan laboratories), GLAST-CreER^{T2} (Mori et al., 2006), Nestin-CreER^{T2} (Corsini et al., 2009), NG2-CreER^{T2} (B6.Cg-Tg/Cspg4-Cre/Esr1*/BAkik/J; Jackson Labs; Zhu et al., 2011), R26R-YFP (Srinivas et al., 2001) and hGFAP-GFP (Zhuo et al., 1997); FVB/N-TgGFAPGFP14Mes/J; Jackson Labs) animals. Nestin-CreER^{T2}, GLAST-CreER^{T2} and NG2-CreER^{T2} were crossed to R26R-YFP mice to produce: Nestin-CreER^{T2}/R26R-YFP and NG2-CreER^{T2}/R26R-YFP mice hemizygous for both genes and GLAST-CreER^{T2}/R26R-YFP mice heterozygous for GLAST-CreER^{T2} and homozygous for R26R:YFP.

Neurosphere assay

Lesioned striatum, healthy striatum and subventricular zone (SVZ; n=4 per experiment) were dissected, dissociated and cultured (10000 cells/mL) in a standard neurosphere assay (Pastrana et al., 2009). For each group the rate of neurosphere generation was determined as the number of primary neurospheres by the number of viable seeded cells. Self-renewal of SVZ and STR-les was determined as the number of neurospheres/number of viable seeded cells derived from spheres of the previous passage. The number of neurospheres was determined after 7 days of culture. Diameters of living neurospheres were measured using ImageJ software. Three replicates were performed. For assessment of differentiation, neurospheres were plated onto polyD-lysine coated coverslip coated in differentiation medium. Plated cells were processed 7 days later using immunocytochemistry: we used anti-GFAP, anti- β III tubulin and anti-O4 to determine astroglial, neuronal and oligodendroglial differentiation, respectively

Quantifications and statistical analyses

All countings were performed in ImageJ on sections acquired at the confocal microscope (voxel size: 0.35 μ m x 0.35 μ m x 1.50 μ m).

Stereological evaluation of the number, organization and BrdU labelling of DCX⁺ and Ki67⁺ cells. This analysis was performed in the six central focal planes of two non-consecutive 50 μ m thick slices. The DCX⁺ and Ki67⁺ clusters were defined as

groups of at least four cells with closely contacting cell bodies and expressing the same marker. For double-labelled cells, clustering has been evaluated separately for each marker.

Expression of ASCL1 (n=2), SOX9 (n=2) and GFAP-GFP (n=3) in striatal cK, cKD, cD, iD cells was evaluated in 3-4 slices. The number of counted cell per animal ranged from 55 to 100 cells for cK, 182 to 206 for cKD. For iD and cD 100 cells per animal were counted.

Genetic fate-mapping analysis of SVZ and striatal cells: Analyses were performed in Nestin-CreER^{T2} (Nestin-CreER^{T2} bQA n=4, Nestin-CreER^{T2} aQA n=5) and GLAST-CreER^{T2} animals (GLAST-CreER^{T2} bQA n=3, GLAST-CreER^{T2} aQA n=3). In the SVZ, the percentage of recombined Ki67⁺/DCX⁻ (K_{SVZ}), Ki67⁺/DCX⁺ (KD_{SVZ}), and Ki67⁺/DCX⁺ (D_{SVZ}) were counted at the level of the rostral migratory stream (RMS) in hemispheres ipsilateral to the lesion. Counted cells ranged from 64 to 165 for K_{SVZ} cells; from 54 to 144 for KD_{SVZ} cells and from 332 to 888 for D_{SVZ} cells). In the striatum, fractions of GFP⁺ cK, cKD, and iD cells were counted over the entire thickness of 2-4 sections while cD cells were counted in two non-consecutive focal planes. Counted cells ranged from 77 to 473 for cK cells, from 85 to 474 for cKD cells, from 82 to 192 for cD cells and from 460 to 1160 for iD cells.

Cell composition of reporter⁺ Ki67⁺ clusters in fate-mapped animals. This analysis was performed on randomly selected Ki67⁺ clusters that contained at least a single reporter⁺ cell. Selected clusters were entirely reconstructed from subsequent sections and the number of reporter⁺ and reporter⁻ cells were counted. The number of Ki67⁺ clusters that were composed by 100% reporter⁺ cells over the total number of analyzed clusters were as follows: GLAST-CreER^{T2} bQA, 35/39; GLAST-CreER^{T2} aQA 21/24 Nestin-CreER^{T2} bQA 8/8, Nestin-CreER^{T2} aQA 20/31; VSVG-GFP 17/18; Ad:GFAP-Cre 11/12.

Statistical analyses were performed in SPSS 19. Anova analyses that returned significant F values were followed by Tukey's post hoc tests.

References

Corsini, N. S., Sancho-Martinez, I., Laudenklos, S., Glagow, D., Kumar, S., Letellier, E., Koch, P., Teodorczyk, M., Kleber, S., Klussmann, S. et al. (2009).

The death receptor CD95 activates adult neural stem cells for working memory formation and brain repair. *Cell Stem Cell* 5, 178-190.

Lowenstein, P. R. and Castro, M. G. (2003). Inflammation and adaptive immune responses to adenoviral vectors injected into the brain: peculiarities, mechanisms, and consequences. *Gene Ther.* 10, 946-954.

Mori, T., Tanaka, K., Buffo, A., Wurst, W., Kühn, R. and Götz, M. (2006). Inducible gene deletion in astroglia and radial glia—a valuable tool for functional and lineage analysis. *Glia* 54, 21-34.

Pastrana, E., Cheng, L.-C. and Doetsch, F. (2009). Simultaneous prospective purification of adult subventricular zone neural stem cells and their progeny. *Proc. Natl. Acad. Sci. USA* 106, 6387-6392.

Srinivas, S., Watanabe, T., Lin, C.-S., Williams, C. M., Tanabe, Y., Jessell, T. M. and Costantini, F. (2001). Cre reporter strains produced by targeted insertion of EYFP and ECFP into the ROSA26 locus. *BMC Dev. Biol.* 1, 4.